

Article

A Study on the Annealing Ambient Effect on the Anti-Pollution Characteristics of Functional Film for PV Modules

Sejin Jung ¹, Jung Hyun Kim ², Jang Myoun Ko ³ and Wonseok Choi ^{1,*}

¹ Department of Electrical Engineering, Hanbat National University, Daejeon 34158, Korea; fractochamel@naver.com

² Department of Advanced Materials Science and Engineering, Hanbat National University, Daejeon 34158, Korea; jhkim2011@hanbat.ac.kr

³ Department of Chemical Engineering and Biotechnology, Hanbat National University, Daejeon 34158, Korea; jmko@hanbat.ac.kr

* Correspondence: wschoi@hanbat.ac.kr; Tel.: +82-42-821-1094

Received: 27 September 2018; Accepted: 13 November 2018; Published: 19 November 2018



Abstract: In this study, functional coating film was fabricated on glass for photovoltaic (PV) modules to improve the anti-pollution characteristics of PV modules. The functional coating film applied to a glass substrate through the spray coating method was annealed at 300 °C for 10 min in H₂, N₂, Ar, O₂, and vacuum ambient. The contact angle of the coated surface was measured and it was confirmed that the anti-pollution characteristics were improved as the contact angle decreased. The light transmittance was measured and it exhibited the most excellent characteristics in vacuum. The hardness and adhesion were measured as the mechanical characteristics and they were all excellent regardless of the annealing ambient. Based on the analyzed characteristics, the process conditions of functional coating films were optimized to improve the anti-pollution and mechanical characteristics. If the coating process optimized in this study is applied to PV modules based on these results, improvement in the anti-pollution characteristics can be expected.

Keywords: anti-pollution; functional film; PV module; annealing ambient

1. Introduction

As the Paris Agreement was signed in 2015 to limit the global temperature increase and to reduce carbon emissions, 195 countries agreed that they would set and implement their own greenhouse gas reduction targets until the launch of the post-2020 climate regime in 2020. Among the renewable energy sources, solar power generation is the most eco-friendly power generation method that does not generate pollution and use fossil fuels. Such solar power generation requires large installation areas to produce a large amount of power and must be installed outdoors to receive sunlight. This causes different performances depending on the installation environment [1–4]. Photovoltaic (PV) modules installed outdoors are exposed to various pollutants, such as yellow dust, bird excrement, and rainfall sediment. Such pollutants reduce the sunlight that enters PV modules and thereby lower power generation efficiency. Therefore, various studies have been underway recently to effectively prevent the surface pollution of PV modules [5,6].

The PV module surface coating materials being researched must have anti-pollution functions and endure severe external temperature differences, as well as external shocks, and they must also endure chemical factors, such as bird's excrement and acid rain. In addition, they must have a light transmittance of 95% or higher [7,8]. Existing solar power plants have been installed in large areas to produce a large amount of power and, thus, a massive amount of time and cost is required for

maintenance, including surface cleaning. Therefore, if pollutants can be easily removed using natural rainfall, the economic efficiency of solar power generation systems will be significantly improved. For the development of a coating material capable of enduring physical and chemical environments, the development of innovative source materials and coating processes are required. Currently, surface self-cleaning coating technology using photocatalysts is available, but this technology has low durability due to its low adhesion and hardness. It also requires energy sources that cause catalysis, and the facility investment cost is low as is demand [9]. In addition, studies have been conducted for decades to prevent fogging on transparent surfaces. One representative method among the methods to address such problems is to modify these surfaces into hydrophilic or hydrophobic surfaces or to apply a coating [10].

As hydrophobic coatings form water droplets in a nearly perfect spherical shape, water droplets remove dust particles from the surface as they roll off. In this case, however, an appropriately rough surface is required and this rough surface may reduce the transmittance by increasing light scattering [11]. On the other hand, a hydrophilic coating removes dust by spreading water on the surface instead of forming water droplets on the surface. This method allows water droplets to spread between pollutants and the substrate surface, thereby removing the pollutants to be attached to the substrate and letting them flow with water droplets [12–16]. The water-soluble polymer materials TiO_2 and silica are known to have excellent hydrophilicity [17]. In this study, we used silica-based material with high light transmittance and durability as a functional material for the anti-pollution function of cover glass for PV modules.

As such, this study aims to propose a new coating process technology that can improve the anti-pollution characteristics of PV modules. First, a hydrophilic silica-based coating material was coated on the surface of cover glass for PV modules and annealed, and then the anti-pollution characteristics were analyzed. In this instance, gas was injected when annealing was performed. The annealing ambient conditions were H_2 , N_2 , Ar, O_2 , and vacuum. For the fabricated functional coating films, the contact angle, anti-pollution characteristics, transmittance, hardness, surface adhesion, and morphological properties were measured.

2. Experimental Section

The coating solution that was used to improve the anti-pollution characteristics of PV modules was an inorganic material that included silicon dioxide (SiO_2), lithium (Li), and potassium (K). The viscosity of the coating solution was 1–3 cP·s, the density was 1.1 g/cm³, and the specific gravity was 1.13 ± 0.05 . The coating solution can be coated on various materials, such as metals, ceramics, and glass. The coating solution used to make the coated film was FC-B106 (Fine-coat, Wellture-Finotech). This solution is a nanosilicon compound that is the basic material of colloidal silica [18].

Prior to coating the functional coating solution on the slide glass substrates, the substrates were subjected to ultrasonic cleaning for 10 min in each of the following solutions: Trichloroethylene, acetone, methanol, and deionized water (D.I. water). The cleaning process performed on the substrate was useful for removing organic and inorganic contaminants from the surface of the glass substrate. The coating solution was coated on the slide glass substrates using a brush. The thickness of the coated film was around 180 nm, depending on the number of coatings. After being dried at room temperature for 20 min, the coated films were annealed in H_2 , N_2 , Ar, O_2 , and vacuum ambient, at a temperature of 300 °C for 10 min using microwave plasma enhanced chemical vapor deposition (MPECVD) to examine characteristics according to the annealing gas types.

The contact angles of the fabricated functional coating films were measured using Phoenix 300 Touch from S.E.O. The hardness was measured using a hardness tester from CORE TECH, Korea, in accordance with ASTM D3363, which is the measurement method of the American Society for Testing Materials (ASTM), and the adhesion was measured using the H-9H, F, HB, and B-6B pencils from Mitsubishi in accordance with ASTM D3359, which is the surface adhesion measurement method of ASTM. The optical characteristics were measured using the integrating sphere of UV-visible

spectroscopy, i.e., Mega 700 from Scinco. The thickness of the coated film was measured using a thickness profilometer (NanoMap-500LS, HTSK). The surface morphologies and roughness of the coated film were measured using atomic force microscope (AFM, XE-100, Park Systems).

3. Results and Discussion

Figure 1 shows the water droplet contact angle characteristics of the naturally-dried functional coating film, as well as the functional coating film annealed in H_2 , N_2 , Ar, O_2 , and vacuum ambient. The contact angle of the naturally-dried film was measured to be 26.1° . The contact angles of the functional coating film annealed in Ar, N_2 , and O_2 ambient ranged from 10.5° to 12.1° . The contact angle of the film annealed in the H_2 ambient was 16.0° . However, the contact angle of the film annealed in the vacuum ambient was 8.6° , indicating the most excellent hydrophilic characteristics.

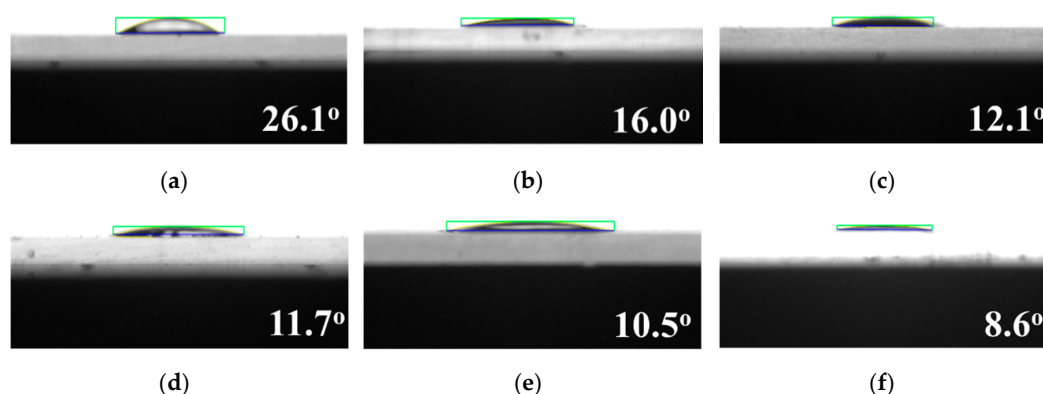


Figure 1. Contact angle of the functional coating film according to the annealing gas; (a) is naturally dried, (b–f) are annealed with H_2 , N_2 , Ar, O_2 , and in a vacuum, respectively.

Figure 2 shows the anti-pollution characteristics of the naturally-dried functional coating film, as well as the functional coating film annealed in H_2 , N_2 , Ar, O_2 , and vacuum ambient. On the slide glass substrates where the film functional coating was formed, black, red, and blue markings were applied using oil pens. As a result of dropping water droplets after naturally drying the markings, the specimen annealed in the vacuum ambient exhibited the most excellent anti-pollution characteristics, as shown in Figure 2. This result is in agreement with the result of contact angle, indicating that the annealing of the functional coating film in the vacuum ambient exhibits excellent anti-pollution characteristics by dropping water.

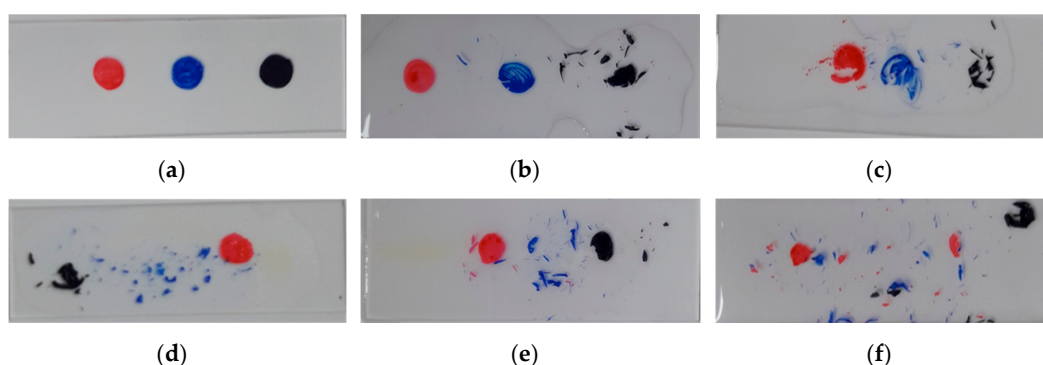


Figure 2. Anti-pollution characteristics of the functional coating film according to the annealing gas, (a) is naturally dried, (b–f) are annealed with H_2 , N_2 , Ar, O_2 , and in a vacuum, respectively.

Figure 3 shows AFM images of the functional coating film measured by AFM. The AFM image shows the roughness of naturally dried functional coating film as well as the functional coating film annealed in the H_2 and vacuum ambient. The roughness of the naturally dried functional coating film,

coating film annealed in the H_2 , and coating film annealed in the vacuum ambient were measured to be 6.53 nm, 3.50 nm, and 1.41 nm respectively. As the roughness decreased, the contact angle of the functional coating film decreased. This result shows that the surface roughness of the film has relations with the hydrophilicity.

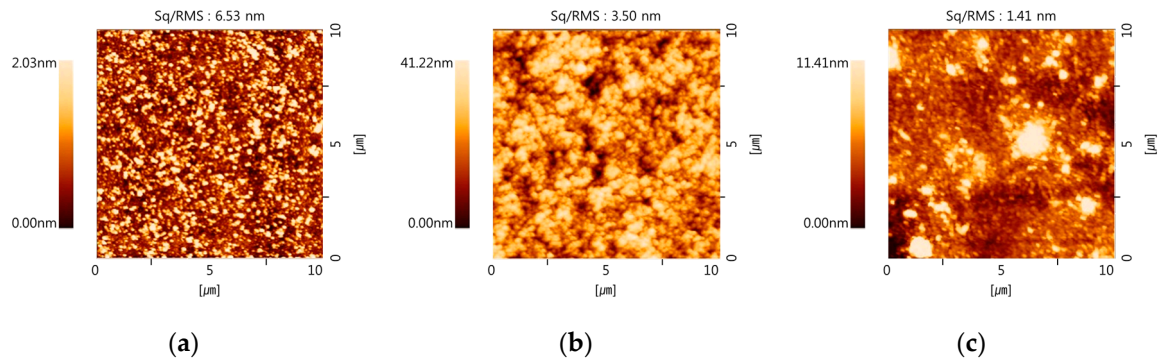


Figure 3. AFM images of functional coating film according to the annealing condition, (a) is naturally dried, (b) is annealed with H_2 , and (c) is annealed in a vacuum.

Figure 4 shows the average light transmittance measured in a wavelength of 400 to 800 nm of the naturally-dried functional coating film, as well as the functional coating film annealed in H_2 , N_2 , Ar, O_2 , and vacuum ambient. The average light transmittance of the naturally dried functional coating film was measured to be 89%, however, it was increased with annealing treatment. The average light transmittance of the film annealed in the Ar, N_2 , and O_2 ambient ranged from 98.5% to 98.7%, and the average light transmittance of the film annealed in the H_2 ambient was measured to be 96.1%. However, the average light transmittance of the film annealed in the vacuum ambient was 99.0%, indicating the most excellent average light transmittance characteristics. The optical properties were generally improved through the annealing process. Especially, it showed that the best optical characteristics were derived from the vacuum ambient. This means that annealing of the functional coating film mainly composed of nanosilica affects the increase of the average light transmittance by decreasing the bandgap of nanosilica energy and removing the impurities of the film. If the film is annealed while gas is being injected, the impurities to be removed by the annealing may be disturbed by the gas. Therefore, it means that the average light transmittance property improves when the film is annealed in a vacuum [19,20].

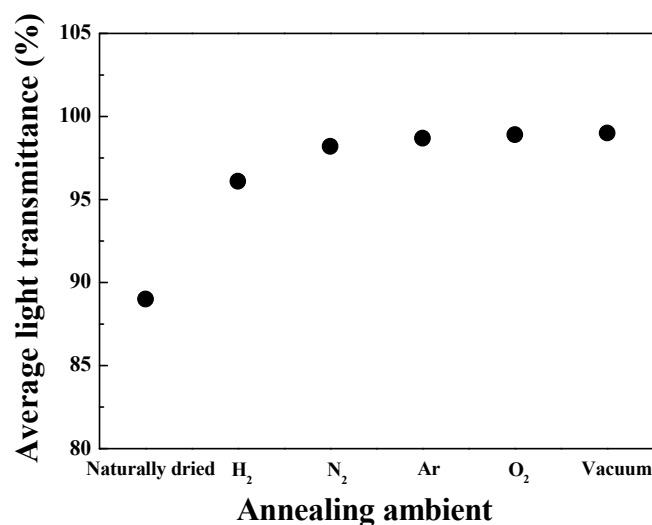


Figure 4. Average light transmittance of the functional coating film according to the annealing method and ambient.

Figure 5 shows the hardness characteristics of the naturally dried functional coating film as well as the functional coating film annealed in Ar, N₂, H₂, O₂, and vacuum ambient. The hardness was measured in accordance with ASTM D3363. The hardness of the naturally-dried functional coating film was 5H. All of the annealed films exhibited excellent hardness characteristics of 9H. It was confirmed that the hardness of the functional films were improved through the annealing process.

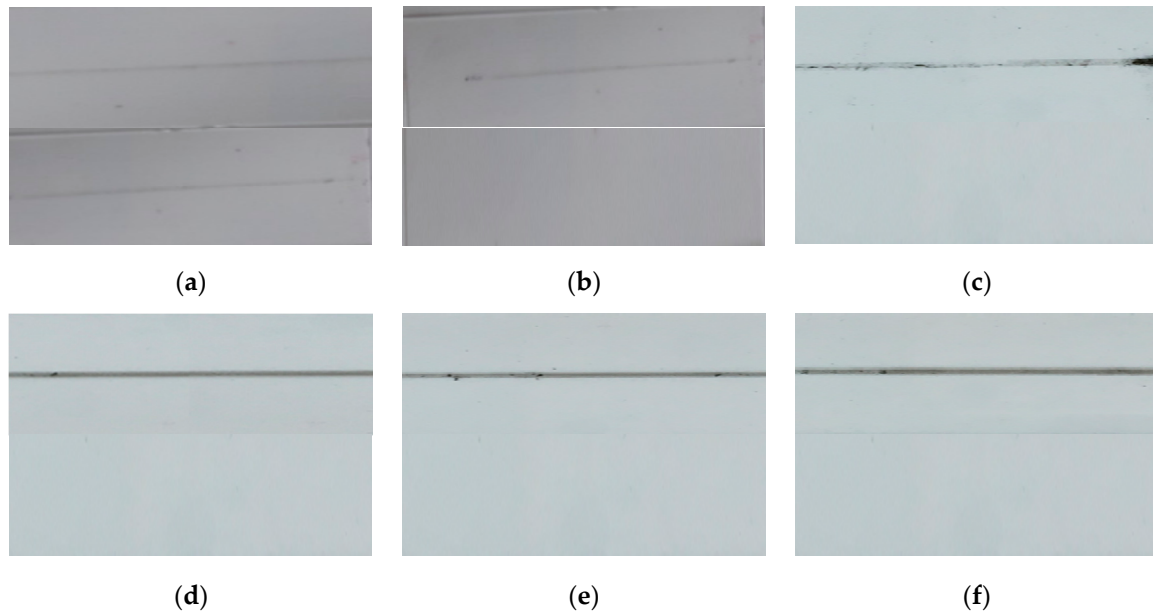


Figure 5. Hardness characteristics of the functional coating film according to the annealing gas, (a) is naturally dried, (b–f) are annealed with H₂, N₂, Ar, O₂, and in a vacuum, respectively.

Figure 6 shows the surface adhesion characteristics of the naturally-dried functional coating film, as well as the functional coating films annealed in H₂, N₂, Ar, O₂, and vacuum ambient. ASTM 3359, which is the surface adhesion measurement method of ASTM, was used. The ASTM D3359 method is the standard test for measuring adhesion and uses a tape test. The measurement results showed that the hardness of the naturally-dried functional coating film was 3 GPa. All of the annealed films exhibited excellent surface adhesion characteristics of 5 GPa. It was confirmed that the adhesion of the functional film was improved through the annealing process.

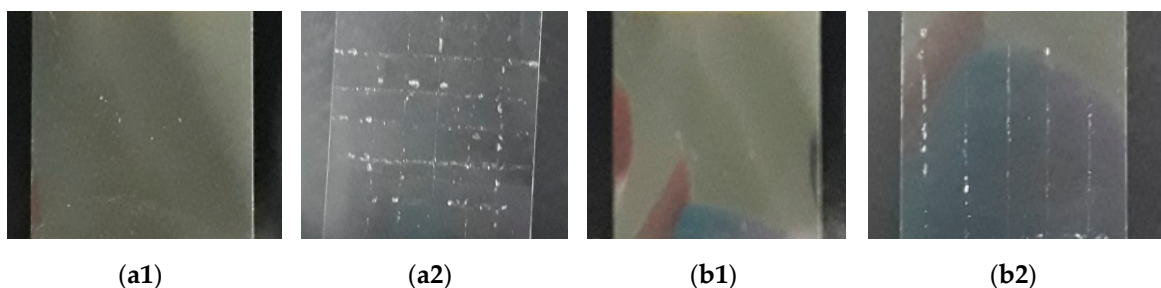


Figure 6. Adhesion characteristics of the functional coating according to the annealing gas, (a1) is tape before the hardness test of the naturally dried film, (a2) is tape after the hardness test of the naturally dried film, (b1) is tape before the hardness test of the annealed film, (b2) is tape after the hardness test of the annealed film.

4. Conclusions

In this study, the characteristics of functional coating films fabricated on glass substrates for PV modules were investigated according to the annealing ambient. To examine characteristics according

to the annealing ambient, the functional coating solution was coated on glass substrates and annealed in H₂, N₂, Ar, O₂, and vacuum ambient. As a result of measuring the contact angle, the film annealed under the vacuum conditions exhibited the lowest contact angle of 8.6°. In addition, the analysis of anti-pollution characteristics through water spraying revealed that all films showed anti-pollution characteristics, and that the sample annealed in a vacuum ambient exhibited the most excellent anti-pollution characteristics. As a result of analyzing light transmittance characteristics, the film annealed in a vacuum ambient exhibited the most excellent optical characteristics. The analysis of hardness and adhesion characteristics revealed that all of the annealed films exhibited the highest grade. AFM measurement results showed the variation of roughness according to the annealing conditions. As the contact angle decreased, the roughness measured by the surface profiler also decreased. Based on these results, if the anti-pollution coating process proposed in this study is applied to PV modules, it is expected that power efficiency will be increased due to improved anti-pollution characteristics and that economic efficiency will be improved in terms of maintenance.

Author Contributions: S.J. performed the analyses and wrote the manuscript; J.H.K. and J.M.K. contributed to the conception of the study. W.C. organized and supervised the main research of the study.

Acknowledgments: This study was supported by Korea Electric Power Corporation (Grant No. R17XA05-01) and Korea Institute of Energy Technology Evaluation and Planning (Grant No. 20184030201900).

Conflicts of Interest: The authors declare no conflict of interest.

References

1. Biryukov, S. An experimental study of the dry deposition mechanism for air-borne dust. *J. Aerosol Sci.* **1998**, *29*, 129–139. [[CrossRef](#)]
2. Mastekbayeva, G.A.; Kumar, S. Effect of dust on the transmittance of low density polyethylene glazing in a tropical climate. *Sol. Energy* **2000**, *68*, 135–141. [[CrossRef](#)]
3. Elminir, H.K.; Ghitas, A.E.; Hamid, R.H.; El-Hussainy, F.M.; Beheary, M.; Abdel-Moneim, K.M. Effect of dust on the transparent cover of solar collectors. *Energy Convers. Manag.* **2006**, *47*, 3192–3203. [[CrossRef](#)]
4. Zaihidee, F.M.; Mekhilef, S.; Seyedmahmoudian, M.; Horan, B. Dust as an unalterable deteriorative factor affecting PV panel's efficiency: Why and how. *J. Renew. Sustain. Energy* **2016**, *65*, 1267–1278. [[CrossRef](#)]
5. Li, X.; Zhou, Y.; Xue, L.; Huang, L. Integrating bibliometrics and roadmapping methods: A case of dye-sensitized solar cell technology-based industry in China. *Technol. Forecast. Soc. Chang.* **2015**, *97*, 205–222. [[CrossRef](#)]
6. Liu, C.; Zhang, X.; Li, J.; He, Y.; Li, Z.; Li, H.; Guo, W.; Xie, W. The role of phosphor nanoparticles in high efficiency organic solar cells. *Synth. Met.* **2015**, *204*, 65–69. [[CrossRef](#)]
7. Isshiki, M.; Sichanugrist, P.; Abe, Y.; Oyama, T.; Odaka, H.; Konagai, M. New method to measure whole-wavelength transmittance of TCO substrates for thin-film silicon solar cells. *Curr. Appl. Phys.* **2014**, *14*, 1813–1818. [[CrossRef](#)]
8. Yu, W.; Shen, L.; Shen, P.; Meng, F.; Long, Y.; Wang, Y.; Lv, T.; Ruan, S.; Chen, G. Simultaneous improvement in efficiency and transmittance of low bandgap semitransparent polymer solar cells with one-dimensional photonic crystals. *Sol. Energy Mater. Sol. Cells* **2013**, *117*, 198–202. [[CrossRef](#)]
9. Wu, M.; Lin, Y.N.; Guo, H.; Ma, T.; Hagfeldt, A. Highly effective Pt/MoSi₂ composite counter electrode catalyst for dye-sensitized solar cell. *J. Power Sources* **2014**, *263*, 154–157. [[CrossRef](#)]
10. Tang, R.; Muhammad, A.; Yang, J.; Nie, J. Preparation of antifog and antibacterial coatings by photopolymerization. *Polym. Adv. Technol.* **2014**, *25*, 651–656. [[CrossRef](#)]
11. Shang, Q.; Zhou, Y. Fabrication of transparent superhydrophobic porous silica coating for self-cleaning and anti-fogging. *Ceram. Int.* **2016**, *42*, 8706–8712. [[CrossRef](#)]
12. Arabatzis, I.; Todorova, N.; Fasaki, I.; Tsesmeli, C.; Peppas, A.; Li, W.X.; Zhao, Z. Photocatalytic, self-cleaning, antireflective coating for photovoltaic panels: Characterization and monitoring in real conditions. *Sol. Energy* **2018**, *159*, 251–259. [[CrossRef](#)]
13. Jesus, M.A.M.L.D.; Neto, J.T.D.S.; Timo, G.; Paiva, P.R.P.; Dantas, M.S.; Ferreira, A.D.M. Superhydrophilic self-cleaning surfaces based on TiO₂ and TiO₂/SiO₂ composite films for photovoltaic module cover glass. *Appl. Adhes. Sci.* **2015**, *3*, 5. [[CrossRef](#)]

14. Malviya, K.D.; Chattopadhyay, K. Temperature-and Size-Dependent Compositionally Tuned Microstructural Landscape for Ag-46 Atom% Cu Nanoalloy Prepared by Laser Ablation in Liquid. *J. Phys. Chem. C* **2016**, *120*, 27699–27706. [[CrossRef](#)]
15. Malviya, K.D.; Srivastava, C.; Chattopadhyay, K. Phase formation and stability of alloy phases in free nanoparticles: Some insights. *RSC Adv.* **2015**, *5*, 35541–35550. [[CrossRef](#)]
16. Malviya, K.D.; Dotan, H.; Yoon, K.R.; Kim, I.D.; Rothschild, A. Rogorous substrate cleaning process for reproducible thin film hematite (α -Fe₂O₃) photoanodes. *J. Mater. Res.* **2016**, *31*, 1565–1573. [[CrossRef](#)]
17. Drelich, J.; Chibowski, E.; Meng, D.D.; Terpilowski, K. Hydrophilic and superhydrophilic surfaces and materials. *Soft Matter* **2011**, *7*, 9804–9828. [[CrossRef](#)]
18. Joung, Y.H.; Choi, W.; Shin, Y.; Lee, M.; Kim, H.; Song, W. Properties Characterization of the Hydrophilic Inorganic Film as Function of Coating Thickness. *J. Korean Phys. Soc.* **2013**, *63*, 246–250. [[CrossRef](#)]
19. Balagurov, L.A.; Yarkin, D.G.; Petrova, E.A.; Orlov, A.F.; Karyagin, S.N. Effects of vacuum annealing on the optical properties of porous silicon. *Appl. Phys. Lett.* **1996**, *69*, 2852–2856. [[CrossRef](#)]
20. Kiselev, V.A.; Polisadin, S.V.; Postnikov, A.V. Variation of optical properties of porous silicon as a result of thermal annealing in vacuum. *Semiconductors* **1997**, *31*, 704–706. [[CrossRef](#)]



© 2018 by the authors. Licensee MDPI, Basel, Switzerland. This article is an open access article distributed under the terms and conditions of the Creative Commons Attribution (CC BY) license (<http://creativecommons.org/licenses/by/4.0/>).